Separation Science and Technology
Publication details, including instructions for authors and subscription information:
http://www.informaworld.com/smpp/title~content=t713708471

Separation of Monovalent Cations by Electrodialysis

John D. Norton[a]; Mark F. Buehler[a]
[a] PACIFIC NORTHWEST LABORATORY, BATTELLE BOULEVARD, RICHLAND, WASHINGTON

To cite this Article Norton, John D. and Buehler, Mark F.(1994) 'Separation of Monovalent Cations by Electrodialysis', Separation Science and Technology, 29: 12, 1553 — 1566
To link to this Article: DOI: 10.1080/01496399408007373
URL: http://dx.doi.org/10.1080/01496399408007373

SEPARATION SCIENCE AND TECHNOLOGY, **29**(12), pp. 1553–1566, 1994

Separation of Monovalent Cations by Electrodialysis

JOHN D. NORTON and MARK F. BUEHLER*
PACIFIC NORTHWEST LABORATORY
BATTELLE BOULEVARD, P.O. BOX 999, RICHLAND, WASHINGTON 99352

ABSTRACT

Electrodialysis has been used to separate sodium and cesium ions in aqueous solution. Experiments utilizing a Nafion 417 cationic membrane and an RAI Raipore R-1030 anionic membrane in a three-compartment cell resulted in an increased flux of cesium over sodium through the cationic membrane. A maximum separation efficiency ranging from 2 to 3 was observed at currents below the mass-transport-limited plateau. At currents above the mass-transport-limited value, the separation efficiency decreased to approximately 1.27, which compared well with that determined by the relative ionic mobilities. When the flow rate of the anolyte, catholyte, and feed was varied, it was shown that the process scaled linearly, which demonstrates the potential for large-scale equivalent ion separation by electrodialysis.

INTRODUCTION

Electrodialysis is a technique commonly used to separate charged species. The process utilizes charge-selective membranes and an applied electric field to facilitate the separation. Many industries have found applications for electrodialysis. Examples of these applications include the production of food-grade salt; desalination of potable water; removal of excess acid from fruit juices; production of chlorine gas and sodium hydroxide; elimination of pollutants from waste streams (i.e., Hg^{+2}, Cd^{2+} or Pb^{2+}); and the demineralization of cheese whey, sugar solutions, and other food products. These applications primarily involve a separation based on a difference in valence state and valence charge.

* To whom all correspondence should be sent.

Electrodialysis may also be designed for specific applications, such as separation of radionuclides from waste streams containing species of equal charge. This paper discusses a method that was evaluated at Pacific Northwest Laboratory to separate sodium and cesium ions in aqueous solution.

The parameters controlling the electrolytic separation are understood by examining the mechanisms of ionic transport. In dilute solutions, the transport of an ionic species, j, is represented by the Nernst–Planck equation:

$$\mathbf{J}j = -D_j \nabla C_j - \frac{z_j F}{RT} D_j C_j \nabla \phi + C_j \mathbf{v} \tag{1}$$

where D_j is the diffusivity of species j, C_j is its concentration, z_j is its valence charge, F is Faraday's constant, R is the universal gas constant, T is the absolute temperature, ϕ is the electrostatic potential, and $\mathbf{v}$ is the fluid velocity vector. The term D_j/RT is referred to as the ionic mobility, u_j. The three terms in Eq. (1) physically represent contributions from diffusion, migration, and convection, respectively. Because electrodialysis utilizes a flow cell, the transport-limiting step occurs within either the stagnant boundary layer adjacent to the membrane surface or within the membrane. Under these flow conditions, the effects of forced and free convection can be neglected. In addition, within the membrane and the boundary layer, the migratory component will greatly exceed the diffusive component at all but the lowest currents.

A simplified diagram of an electrodialysis cell used for the splitting of an aqueous sodium nitrate solution is shown in Fig. 1. The cell consists of three compartments, the anolyte, the feed, and the catholyte, with anionic and cationic permselective membranes separating the feed from the anolyte and catholyte, respectively. When a suitably high potential is applied across the cell, water is oxidized at the anode to produce protons and reduced at the cathode to produce hydroxyl ions:

$$\text{Anode:} \quad 2H_2O \rightleftharpoons O_2(g) + 4H^+ + 4e^- \tag{2}$$

$$\text{Cathode:} \quad 4H_2O + 4e^- \rightleftharpoons 2H_2(g) + 4OH^- \tag{3}$$

The resultant electric field across the cell causes the migration of nitrate through the anionic membrane toward the anode to form nitric acid and the migration of sodium through the cationic membrane toward the cathode to form sodium hydroxide. The protons and hydroxyl ions produced at the electrodes are confined to the cells in which they are generated by the anionic and cationic membranes. The net result of this process is separation of salt ions from the feed stream and the production of an acidic anolyte and basic catholyte stream.

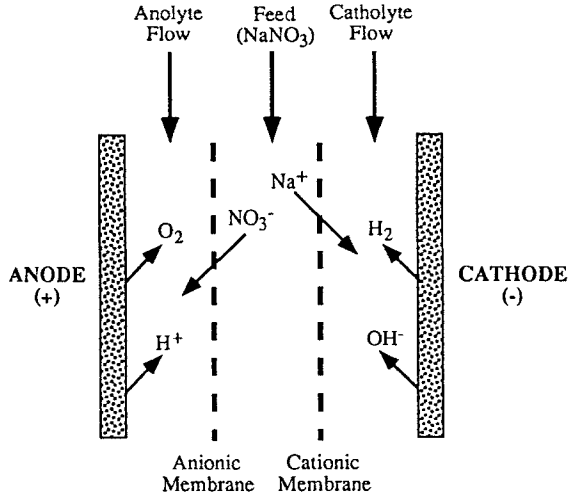

FIG. 1 Simplified schematic of ion movement during an electrodialytic salt separation process.

The use of electrodialysis for the separation of species of equal charge and valence was studied here as a possible treatment technique for use in environmental remediation of the U.S. Environmental Protection Agency's Superfund Sites and, specifically, the Hanford Site in Richland, Washington.

There are 177 underground storage tanks at the Hanford Site that contain approximately 61 million gallons of high-level radioactive waste. Typical waste streams from these tanks contain relatively low concentrations of radioactive species such as $^{137}Cs^+$ and high concentrations of Na^+. The current disposal strategy is to separate the tank waste into high-level and low-level radioactive waste. The high-level waste will be stabilized in a borosilicate glass matrix through an expensive process called vitrification, whereas the low-level waste will be immobilized inexpensively in a cement grout. If the radioactive ions can be preferentially concentrated from the waste stream prior to final disposal, the volume of high-level waste can be decreased, allowing more material to be economically disposed of as low-level waste.

The primary advantage of using electrodialysis for this type of separation is that secondary waste is not generated as in other separation techniques such as ion exchange, solvent extraction, and precipitation. In addition, acid and base streams generated during the process may be used

elsewhere in the tank remediation process, and the technique is applicable over a large pH range (0–14). A further advantage is that the driving force for the separation, the applied electric field, can be controlled instantly and accurately.

This study examines the feasibility of using electrodialysis to separate monovalent cations, specifically, aqueous Na^+ and Cs^+ ions. For this application, cesium nitrate is added to the feed stream in Fig. 1. The relative separation of sodium and cesium ions from the feed to the catholyte stream will then be determined by their ionic mobilities and the selectivity of the cationic membrane.

EXPERIMENTAL APPARATUS AND PROCEDURE

The experimental apparatus consists of an electrodialysis cell, a central pumping unit, flowmeters, and a potentiostat. Figure 2 shows a schematic of the experimental system. An ElectroCell AB Micro Flow Cell (Electrosynthesis Co., Inc., Lancaster, New York) was used to perform electrodialysis experiments. The micro-flow cell was operated in a three-compartment configuration with parallel flat-plate electrodes. The electrode materials were a nickel cathode and a dimensionally stable anode designed for O_2 evolution in low pH solutions. A spacer with a mesh flow distributor was inserted into each compartment to provide a uniform and reproducible flow field for all experiments. A Nafion 417 cationic membrane was used for the Na^+/Cs^+ separation, and an RAI Raipore R-1030 anionic membrane was used to prevent the migration of protons to the catholyte compartment. Inert Kynar gaskets were used to ensure leak-tight seals around the membranes, spacers, and electrodes.

Each electrode or membrane had an exposed area of 10 cm^2, resulting in approximately 1.5 cm^3 for the volume of each compartment. The system was operated in a one-pass mode without recycling. The anolyte, catholyte, and feed solutions were pumped from their reservoirs to their respective cell compartments with a MasterFlex Model 7567 pump unit (Cole Palmer, Niles, Illinois). The unit was capable of driving three peristaltic pump heads simultaneously on a single drive shaft. The system tubing material was primarily PFA Teflon with the exception of a small portion within the pump heads, which was Tygon R-3603. Gilmont (Barrington, Illinois) direct reading flowmeters of glass and PTFE Teflon were installed on the inlets and outlets of the cell, and minor flow adjustments were made with micrometer valves on the downstream side. This ensured that all three compartments had equal pressure drops, thereby decreasing the possibility of crossflow between compartments.

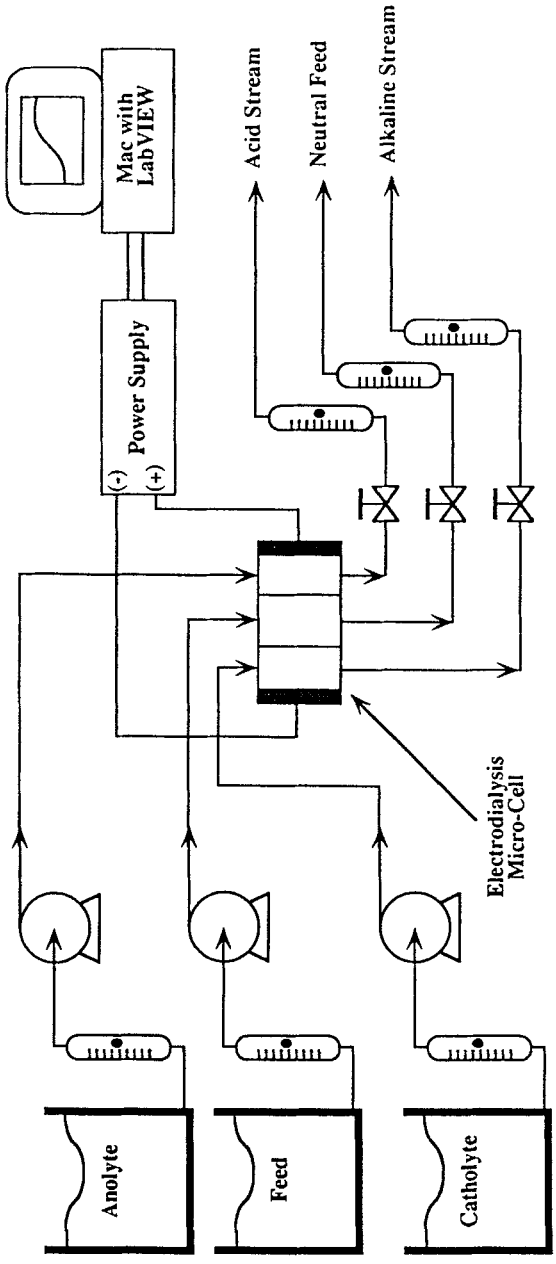

FIG. 2 Block diagram of the experimental apparatus used to separate mixtures of Na^+ and Cs^+.

The electrical driving force for the ion separation was provided by a PAR Model 175 Universal Programmer in conjunction with either a PAR Model 173 or Model 371 Potentiostat/Galvanostat (EG&G, Princeton, New Jersey). The Model 173 was used for Na^+/Cs^+ concentration ratios of 1 and 10, while the Model 371 was necessary for the ratio of 100 because of the large currents generated. All experiments were run in a traditional linear or cyclic voltammetric procedure. The Model 175 was used to vary the potential from approximately 2 to 9 V at scan rates ranging from 1 to 5 mV/s. The voltage and current data were collected by a Macintosh IIcx computer through an analog-to-digital board (National Instruments, NB-MIO-16H, Austin, Texas). The data acquisition board was 12-bit, corresponding to a resolution of 2.44 mV. The computer acquisition rate was approximately 1.5 seconds and was controlled using LabVIEW2 software (National Instruments, NB-MIO-16H, Austin, Texas).

Sodium nitrate (ACS, Aldrich, Milwaukee, Wisconsin), cesium nitrate (99.999%, Aldrich), potassium hydroxide (AR, Mallinkrodt, Paris, Kentucky), and nitric acid (AR, Mallinkrodt) were used as received. All solutions were prepared with 18.2 MΩcm water (Milli-Q UV Plus, Millipore C .p., Bedford, Massachusetts).

Initially, all three compartments were pumped with 18 MΩcm water to balance the flows and check for leaky seals. The reservoirs were then switched to the appropriate solutions and pumping resumed. Samples from each of the effluent streams (anolyte, catholyte, and feed) were separately collected from midstream. The total volume collected was typically 10 mL and varied slightly, depending on the operating flow rate.

An Instrumentation Laboratory 451 AA/AE Spectrophotometer was used to determine the sodium and cesium concentrations in each effluent stream. Atomic emission was used to measure the sodium concentration, while atomic absorption was used to quantify cesium. The error in each measurement was estimated to be 4% and was dominated by the instrument error.

RESULTS AND DISCUSSION

Figure 3A shows a representative cyclic voltammogram for an electrodialysis experiment with an aqueous feed solution of 10 mM $NaNO_3$ and 10 mM $CsNO_3$. The anolyte and catholyte consisted of 56 mM solutions of HNO_3 and KOH, respectively. Each solution was pumped at a rate of 5 mL/min, and the voltage was ramped at 1 mV/s. Little hysteresis was observed in the reverse scan, and increasing the scan rate by as much as a factor of 5 had no noticeable effect. The voltammogram exhibits the characteristic S-shape observed for mass-transfer limited systems (1–3).

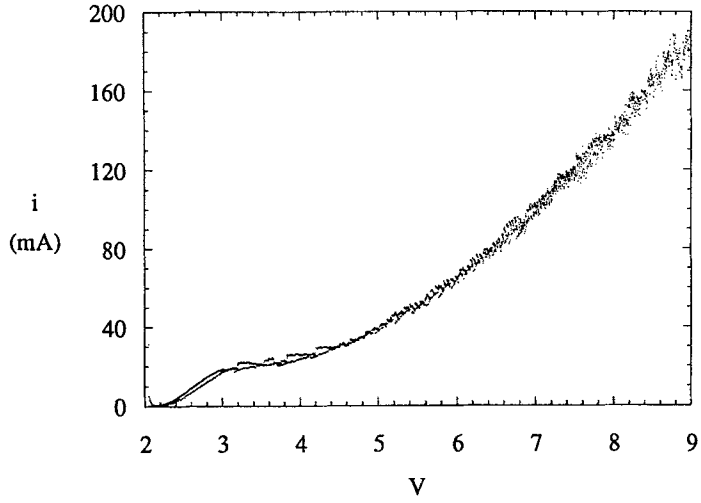

FIG. 3A Cyclic voltammogram for an electrodialysis experiment involving an aqueous feed solution of 10 mM $NaNO_3$ and 10 mM $CsNO_3$ at a flow rate of 5 mL/min.

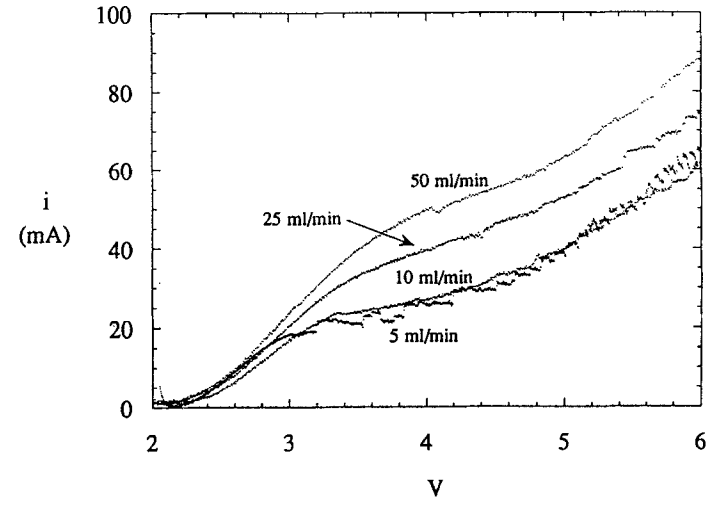

FIG. 3B Current versus voltage response for flow rates of 5, 10, 25, and 50 mL/min.

The curve contains three distinct regions in which different mechanisms control the current. In the first region, the behavior is approximately ohmic, corresponding to the existence of a quasi-equilibrium state at the interface between the membrane and the solution. This is followed by a second region where a "transport-limited" current plateau is observed. In this situation, the current is limited by the rate of mass transfer across the stagnant boundary layer adjacent to the membrane surface, with the concentrations of the species that carry charge through the membrane approaching zero at the membrane surface. The final region is characterized by a rapid current increase with increasing voltage and a corresponding increase in signal noise. The cause of this behavior has been the subject of several studies (4–14). Initial reports (4–8) postulated that the current increase is due to the oxidation and reduction of water at the membranes. However, more recent results indicate that the phenomenon may be caused by a breakdown in electroneutrality adjacent to the membrane surface (9–12), or a combination of the two effects (13, 14).

Increasing the flow rate to 10, 25, and 50 mL/min resulted in the behavior shown in Fig. 3B. As the fluid velocity increased, the transport-limited current increased from 18 mA to 24, 36, and 50 mA, approximately with the square root of the velocity. Such behavior is expected. In the transport-limited current region the rate of mass transfer across the boundary layer will vary linearly with the boundary layer thickness (15) which, in turn, varies with the square root of the fluid velocity, as determined by Blasius (16).

In industry, a wide variety of electrochemical cell geometries, electrodes, and flow patterns are used. Normally, the flow fields are too complex to warrant exact numerical solutions for the velocity profiles by fluid mechanics. Instead, expressions are sought that use space-averaged quantities while permitting insight into the mass transfer characteristics. A very useful method using this logic is dimensional analysis.

Dimensional analysis provides correlations that express the mass transport characteristics in terms of the fluid flow conditions and the electrolyte properties. A correlation describing mass transport by convective-diffusion, neglecting free convection, is given below:

$$\mathrm{Sh} = a\mathrm{Re}^{b}\mathrm{Sc}^{c} \tag{4}$$

where

$$\mathrm{Sh} = k_{\mathrm{m}}\, d_{\mathrm{e}}/D \tag{5}$$

$$\mathrm{Re} = d_{\mathrm{e}} v \rho/\mu \tag{6}$$

$$\mathrm{Sc} = \mu/D\rho \tag{7}$$

$$k_m = \frac{J}{c_\infty - c_s} = \frac{i_{lim}}{zFA(c_\infty - c_s)} \tag{8}$$

a, b, and c are empirical constants; Sh is the Sherwood number; k_m is the mass-transfer coefficient; d_e is the characteristic length; D is the diffusivity of the species of interest in solution; Re is the Reynolds number; v is the fluid velocity; ρ is the fluid density; μ is the fluid viscosity; Sc is the Schmidt number; J is the flux across the membrane; c_∞ and c_s are the bulk and surface concentrations, respectively; i_{lim} is the mass-transport limited current; and A is the active electrode area. The value of the Sc exponent is typically taken to be $\frac{1}{3}$, based on hydrodynamic theory. A log-log plot of the Sherwood number versus the Reynolds number will provide the constants a and b. Figure 4 shows such a plot using the following parameters: $c_\infty = 20$ mM, $c_s = 0$, $\mu = 0.01$ g/cm·s, $\rho = 1$ g/cm^3, $D = 1.70 \times 10^{-5}$ cm^2/s [the molar average for sodium and cesium (17)], and $d_e = 0.375$ cm [the equivalent diameter of the flow cell (18)]. The plot indicates a relationship of:

$$\mathrm{Sh} = 1.0\mathrm{Re}^{0.44}\mathrm{Sc}^{1/3} \tag{9}$$

Walsh has tabulated numerous correlations for parallel flat-plate flow cells, and the fitted constants obtained here agree well with the expected values (19).

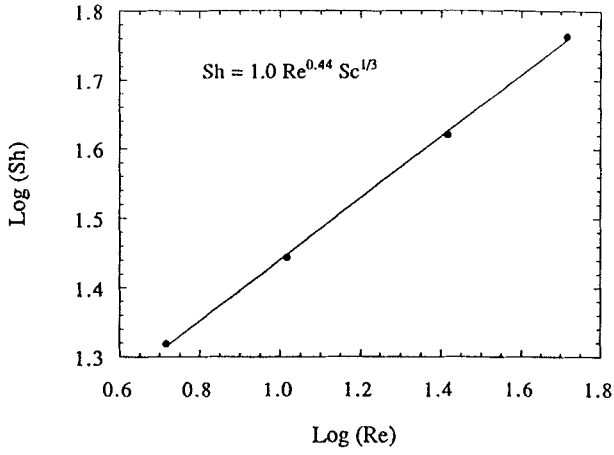

FIG. 4 Log-log plot of the Sherwood number versus the Reynolds number: $c_\infty = 20$ mM, $c_s = 0$, $\mu = 0.01$ g/cm·s, $\rho = 1$ g/cm^3, $D = 1.70 \times 10^{-5}$ cm^2/s, and $d_e = 0.375$ cm.

The ratio of the fraction of cesium that passed through the membrane to the fraction of sodium that passed through the membrane is defined as the separation efficiency, α:

$$\alpha = \frac{[Cs^+_{Catholyte}]/[Cs^+_{Feed}]}{[Na^+_{Catholyte}]/[Na^+_{Feed}]} \tag{10}$$

where $[Cs^+_{Catholyte}]$ is the concentration of Cs^+ in the catholyte effluent, $[Cs^+_{Feed}]$ is the concentration of Cs^+ in the entering feed, $[Na^+_{Catholyte}]$ is the concentration of Na^+ in the catholyte effluent, and $[Na^+_{Feed}]$ is the concentration of Na^+ in the entering feed. Figure 5 shows the separation efficiency plotted as a function of the current normalized to the transport-limited current. For each flow rate, a maximum α value of 2 to 3 occurs at currents below the transport-limited value, indicating the cationic membrane is preferentially allowing Cs^+ to transport into the catholyte. At currents above the transport-limited value, α decays to a constant value ranging between 1.2 and 1.3.

This behavior is consistent with that observed by Rubinstein in an investigation of valency-induced counterion selectivity of ion-exchange membranes (20). At currents below the transport-limited value, the membrane composition is near its quasi-equilibrium value and the system selectivity is predominantly membrane-determined. At higher currents, the higher

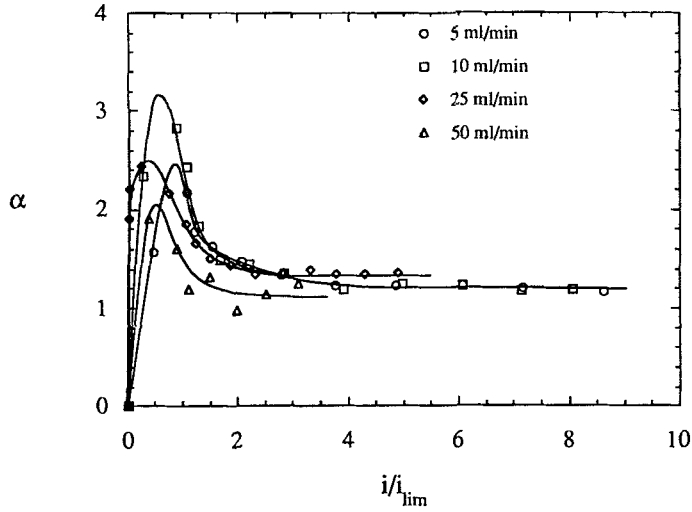

FIG. 5 Separation efficiency as a function of the current normalized to its transport-limited value for flow rates of 5, 10, 25, and 50 mL/min.

flux of Cs^+ through the membrane leads to its depletion in the stagnant boundary layer and a corresponding shift in the equilibrium Cs^+ concentration in the membrane. The result is a decrease in the membrane selectivity. As the current increases further, both Cs^+ and Na^+ are strongly depleted from the boundary layer, and transport across the boundary layer becomes the limiting step of the process. Under these conditions, most membrane selectivity is lost and the separation efficiency is determined by the relative mobilities of Cs^+ and Na^+. A comparison of the diffusivities of Cs^+ and Na^+ (17) shows good agreement between the experimental (1.2 to 1.3) and theoretical (1.27) values of α at currents above the transport-limited plateau.

The effect of increasing the sodium nitrate concentration relative to that of the cesium nitrate is shown in Fig. 6, with the separation efficiency plotted versus the normalized current. It is observed that the separation efficiency decreases slightly as the sodium nitrate concentration increases. However, the α values fall within the same range as those in Fig. 5. As with the previous data, the maximum separation efficiency occurs prior to the transport-limited current plateau.

As previously mentioned, numerous studies have focused on understanding the cause of the current increases beyond the transport-limited

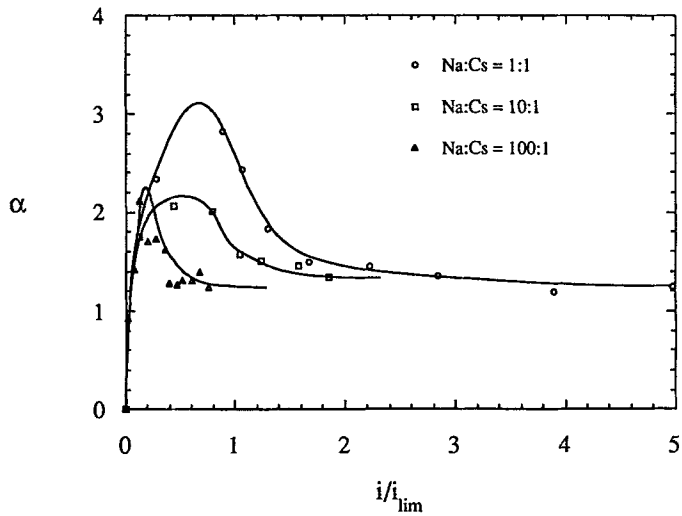

FIG. 6 Separation efficiency as a function of the limiting current normalized to its transport-limited value for Na^+/Cs^+ concentration ratios of 1, 10, and 100; a Cs^+ concentration of 10 mM; and a flow rate of 10 mL/min.

plateau. This question is addressed here by calculating the current efficiency, ϵ, defined as the fraction of current passing through the membrane that is carried by the sodium, i_{Na^+}, and cesium, i_{Cs^+}, ions:

$$\epsilon = \frac{i_{Na^+} + i_{Cs^+}}{i_{total}} \tag{11}$$

where

$$i_{Na^+} = qF[Na^+_{Catholyte}] \tag{12}$$

$$i_{Cs^+} = qF[Cs^+_{Catholyte}] \tag{13}$$

i_{total} is the total current passed, and q is the volumetric flow rate. Figure 7 shows the current efficiency as a function of the normalized current for a flow rate of 10 mL/min, and Na^+ and Cs^+ concentrations of 10 mM. Similar behavior is observed for the other experiments.

If the rapid current increase beyond the limiting value was exclusively due to water splitting, the current efficiency of Na^+ and Cs^+ would decrease at currents above the transport-limited plateau. Throughout the range of currents measured, the current efficiency was relatively constant at 0.60 to 0.65. This implies the increased current results from a propor-

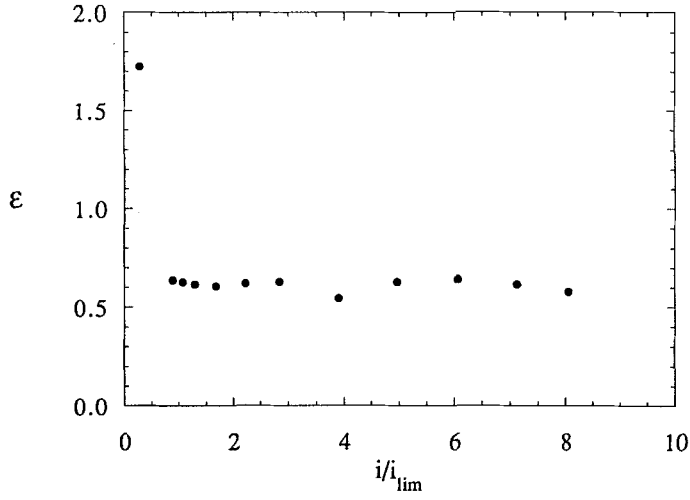

FIG. 7 Current efficiency of Na^+ and Cs^+ as a function of the current normalized to its transport-limited value for a solution of 10 mM $NaNO_3$ and 10 mM $CsNO_3$ and a flow rate of 10 mL/min.

tional increase in each of the ion fluxes across the membrane, rather than water splitting at the membrane. Another possible explanation for the increased current is the physical breakdown of the membrane. However, the lack of hysteresis in the cyclic-voltammogram shown in Fig. 3A suggests that this does not occur.

The one data point in Fig. 7 that does not fall in the 0.60 to 0.65 range is the first at $i/i_{lim} = 0.28$. For this lower current, it is believed that the contributions of the diffusive flux across the membrane and/or leakage around it are comparable to the migratory flux, resulting in an apparent efficiency of greater than unity. This is supported by the presence of Na^+ and Cs^+ in the anolyte stream at concentrations comparable to those necessary to cause the excess efficiency.

CONCLUSIONS

Electrodialysis has been shown to be an effective method for the separation of monovalent cations, specifically, sodium and cesium ions in aqueous solution. The greatest degree of separation occurred at currents below the transport-limited current plateau when the flux is limited by the rate of transport across the membrane rather than across the stagnant boundary layer. At these currents the flux of cesium across the membrane was two to three times greater than that of sodium. The magnitude of the separation efficiency remained essentially constant for $[Na^+]/[Cs^+]$ concentration ratios up to 100. This results suggests that the separation efficiency of the system is membrane-specific, allowing different separations of equal valent ions to be performed by different membrane pairs. The current efficiency for sodium and cesium remained constant for currents up to eight times the transport-limited value. This information provides insight into the mechanisms that contribute to the rapid increase in current beyond the limiting current. For the system examined here, the increased current resulted from an increase in sodium and cesium flux across the cationic membrane and not exclusively from water splitting at the membrane.

The electrodialysis system was characterized by a dimensional analysis to enable scale-up. The mass transfer characteristics were shown to behave similarly to other parallel flat-plate configuration systems. The empirical expression presented demonstrated that large-scale equivalent ion separation by electrodialysis is readily achievable. Finally, the flexibility of electrodialysis demonstrated here opens the possibility of applying electrodialysis to a wide variety of systems through the judicious choice or design of specific ion-selective membranes.

ACKNOWLEDGMENTS

The work described in this paper was supported by the U.S. Department of Energy (DOE). Pacific Northwest Laboratory is operated for DOE by Battelle Memorial Institute under Contract DE-AC06-76RLO 1830.

REFERENCES

1. F. Helfferich, *Ionenaustauscher*, Verlag Chemie CHBH, Weinheim Bergstr., 1959.
2. K. S. Spiegler, *Desalination*, *9*, 367 (1971).
3. C. Forgaces, N. Ishibashi, J. Leibovitz, J. Sinkovic, and K. S. Spiegler, *Ibid.*, *10*, 181 (1972).
4. N. W. Rosenberg and C. E. Tirrell, *Ind. Eng Chem.*, *49*. 780 (1957).
5. H. P. Gregor and M. A. Peterson, *J. Phys. Chem.*, *68*, 2201 (1964).
6. M. Block and J. A. Kitchener, *J. Electrochem. Soc.*, *113*, 947 (1966).
7. J. F. Brady and J. C. R. Turner, *J. Chem. Soc., Faraday Trans. 1*, *74*, 2839 (1978).
8. A. J. Makai and J. C. R. Turner, *Ibid.*, *74*, 2850 (1978).
9. I. Rubinstein and L. Shtilman, *J. Chem. Soc., Faraday Trans. 2*, *75*, 231 (1979).
10. I. Rubinstein and L. A. Segel, *Ibid.*, *75*, 936 (1979).
11. I. Rubinstein, *Ibid.*, *77*, 1595 (1981).
12. I. C. Bassignana and H. Reiss, *J. Phys. Chem.*, *87*, 136 (1983).
13. M. Taky, G. Pourcelly, F. Lebon, and C. Gavach, *J. Electroanal. Chem.*, *336*, 195 (1992).
14. M. Taky, G. Pourcelly, and C. Gavach, *Ibid.*, *336*, 171 (1992).
15. F. Helfferich, *Ion Exchange*, McGraw-Hill, New York, 1962, Ch. 8.
16. H. Blasius, *Z. Math. Phys.*, *56*, 1 (1908).
17. H. S. Harned and J. A. Shropshire, *J. Am. Chem. Soc.*, *80*, 2618, 2967 (1958).
18. J. G. Knudsen and D. L. Katz, *Fluid Dynamics and Heat Transfer*, McGraw-Hill, New York, 1958.
19. F. Walsh, *A First Course in Electrochemical Engineering*, The Electrochemical Consultancy Ltd., England, 1993.
20. I. Rubinstein, *J. Chem. Soc., Faraday Trans. 2*, *80*, 335 (1984).

Received by editor November 11, 1993